AoI Minimization for WSN Data Collection With Periodic Updating Scheme

Guangyang Zhang, *Graduate Student Member, IEEE*, Chao Shen, *Member, IEEE*, Qingjiang Shi, *Member, IEEE*, Bo Ai, *Fellow, IEEE*, and Zhangdui Zhong, *Fellow, IEEE*

***Abstract*— In this paper, we consider the design of a wireless sensor network (WSN) that aims at monitoring the environment and collecting data periodically. In view of the limited energy and computational capability of the sensor nodes, a mobile edge computing (MEC) server is deployed in the WSN as a data processing unit. The goal of the design is to maintain the freshness of the data, which is characterized by the criterion of the age of information (AoI). Therefore, we analyze the long-term average AoI of the considered network. Then, the energy and time constraints for the WSN are modeled with consideration of transmission and computation. Next, a non-convex average AoI minimization problem is formulated subject to the energy and time constraints by jointly optimizing the sampling rate, computing scheduling, and transmit power. To tackle the challenging problem, the geometric programming and successive convex approximation (SCA) technique are applied to develop an algorithm with convergence guarantee. Moreover, to exhibit the benefits of the MEC server, a joint design is investigated for the WSN without the MEC server. Finally, the numerical results demonstrate the efficiency of our proposed SCA-based algorithm and show the impact of the sampling rate on the AoI performance.**

***Index Terms*— Wireless sensor network (WSN), age of information (AoI), mobile edge computing (MEC), sampling rate.**

Manuscript received 28 December 2021; revised 4 May 2022; accepted 9 July 2022. Date of publication 21 July 2022; date of current version 9 January 2023. This work was supported in part by the National Key Research and Development Program of China under Grant 2017YFE0119300; in part by the State Key Laboratory of Rail Traffic Control and Safety, Beijing Jiaotong University, under Contract RCS2021ZP002; and in part by the NSFC, China under Grant 61871027, Grant 62031008, and Grant U1834210. The work of Qingjiang Shi was supported in part by the NSFC under Grant 61671411, Grant 61731018, and Grant U1709219. The work of Zhangdui Zhong was supported in part by the Fundamental Research Funds for the Central Universities under Grant 2022JBXT001; in part by NSFC under Grant 62101026 and Grant 62171021; and in part by the Project of China State Railway Group under Grant SY2021G001 and Grant P2021G012. The associate editor coordinating the review of this article and approving it for publication was K. Choi. *(Corresponding author: Chao Shen.)*

Guangyang Zhang is with the State Key Laboratory of Rail Traffic Control and Safety, Beijing Jiaotong University, and also with Frontiers Science Center for Smart High-speed Railway System, Beijing 100044, China (e-mail: guangyangzhang@bjtu.edu.cn).

Chao Shen is with the State Key Laboratory of Rail Traffic Control and Safety, Beijing Jiaotong University, Beijing 100044, China, and also with the Shenzhen Research Institute of Big Data, Shenzhen 518172, China (email: chaoshen@bjtu.edu.cn).

Qingjiang Shi is with the School of Software Engineering, Tongji University, Shanghai, China, and also with the Shenzhen Research Institute of Big Data, Shenzhen 518172, China (email: shiqj@tongji.edu.cn).

Bo Ai and Zhangdui Zhong are with the State Key Laboratory of Rail Traffic Control and Safety, Beijing Jiaotong University, Beijing 100044, China, and also with Beijing Engineering Research Center of High-speed Railway Broadband Mobile Communications, Beijing Jiaotong University, Beijing 100044, China (e-mail: boai@bjtu.edu.cn; zhdzhong@bjtu.edu.cn).

Color versions of one or more figures in this article are available at https://doi.org/10.1109/TWC.2022.3190986.

Digital Object Identifier 10.1109/TWC.2022.3190986

I. Introduction

RECENTLY, the digital twin (DT) technology widely attracts both the academia and industry attentions. The DT is not only a mirror model of the physical world, but also an evolving system that can understand, predict, and optimize the counterparts of the real world [1]–[4]. Wireless communication plays a fundamental role in building the DT network by supporting the information exchange [2]. To create the virtual twin of a physical object, the DT needs to collect the state information of the object first and then process it. More importantly, the information should be fresh enough to characterize the physical object accurately.

The wireless sensor network (WSN) has proven to be a feasible and practical technology in habitats monitoring, environment protection, and intrusion detection [5]–[9]. In light of this, the WSN is envisioned to enable the DT technology to sense and understand the physical object. Generally, the WSN consists of a sink node and plenty of sensor nodes that monitor the surrounding environment, generate data packets, execute preprocessing, and then deliver the processed packets to the sink node [10]. However, the size-constrained sensor node is usually powered by batteries, which results in limited lifetime and performance degradation of a WSN. Specifically, when some sensor nodes run out of their energy, the information of corresponding zones can no longer be collected. Besides, for a WSN with a large number of sensor nodes, it is impractical to replace batteries with frequent human intervene.

In recent years, mobile edge computing (MEC) has been considered as an essential technique to address the issues of limited computation power and energy for mobile devices [11]–[13], especially in applying the DT [4]. By offloading the computational tasks to the MEC server and balancing the local and remote computation, the latency of the whole network can be reduced significantly. The authors in [14] investigated a tradeoff between energy consumption and latency by jointly optimizing the radio and computational resources. Besides, in [15], the authors took the energy

efficiency and delay into account of a MEC system, where the users can harvest the energy from a power beacon.

Fueled by the potential of the MEC to resolve computation and latency issues, the integration of MEC and WSN is expected to enhance the latency performance of the WSN. On the one hand, with the aid of the MEC server, some energy-intensive processing tasks can be executed at the MEC server by designing the offloading policy instead of processing all the packets locally. On the other hand, due to the introduction of the MEC server, the energy consumption of the sensor node for computation can be reduced. In consequence, by utilizing the saved energy, the nodes can collect data at a higher frequency, thereby decreasing the latency.

In many scenarios, we are concerned about the occurrence of some anomalies in a given area and desire to obtain the information collected by the sensor nodes as timely as possible. It implies that once an abnormality occurs, the sensor node should sense the environment as soon as possible to obtain the freshest information. In order to measure the timeliness of information, we focus on the age of information (AoI), which is a metric of information freshness and attracts much attention of researchers [16]–[20]. Recently, some efforts have been endeavored to enhance the performance of WSNs from the view of AoI [21]–[26]. In [22], the authors studied the performance of a cognitive WSN in terms of AoI and proposed a joint framing and scheduling policy that aims at optimizing the energy efficiency of WSN subject to the average AoI constraint. For an energy harvesting WSN employing time-division multiple access, the authors in [23] aimed to minimize the average AoI of the network by optimizing the resource allocation. In [24], a closed-form expression of average AoI of a WSN equipped with an energy harvested node is derived with consideration of the capacitor's size. Besides, the authors in [25] considered a WSN with sensor nodes transmitting data packets by contending for channel access, and provided a worst-case AoI performance analysis of a M/G/1 queue. In a vehicular network, [26] proposed a cache-assisted lazy update and delivery scheme to well balance the metrics of AoI and service latency.

Motivated by the DT network requirement of the fresh information, in this paper, we consider an integration of the MEC and WSN aiming to minimize the average AoI of the whole network by jointly designing the offloading decision, sampling rate, and transmission power. We assume that the frequency division multiple access (FDMA) technique is applied to the WSN. Besides, the WSN operates with an interval sensing scheme, which means each sensor node senses the environment and generates data packets periodically. Based on the offloading decision, the packets are process locally or at the remote MEC server. With consideration of the energy and computation power constraints, we formulate a non-convex optimization problem aiming at minimizing the long-term average AoI of the WSN. The main contributions are listed as follow.

- Firstly, based on the requirement of considered WSN, we propose a more practical definition of AoI. The proposed AoI characterizes the inherent freshness of the collected data, where the staleness of data derives from the sampling lag and transmission outage. By taking the sampling rate and transmission power into account, we provide a comprehensive analysis of the long-term average AoI of the network, and obtain a closed-from mathematical expression.
- Then, we model the energy of the sensor node and MEC server and time constraints with consideration of the transmission and the computation. A non-convex optimization problem is formulated aiming to minimize the average AoI of the network by optimizing the offloading decision, sampling rates, and transmit power jointly. As a comparison, an average AoI minimization problem for the WSN without the aid of the MEC server is also formulated.
- To treat the non-convex challenge due to the variable coupling, we leverage the technique of geometric programming and then apply the successive convex approximation (SCA) method to solve the AoI minimization problem approximately. The convergence can be guaranteed by the proposed algorithm. In the meanwhile, a closed-form solution is derived for the scenario where the WSN has no MEC server.
- Finally, extensive simulation results are provided to evaluate the performance of our proposed algorithm. The impact of some main parameters on the AoI is also investigated. Moreover, we show that there is a significant positive effect on the AoI performance by integrating the MEC technique with the WSN.

The rest of paper is organized in the following way. Section II introduces the system model of the WSN. Section III gives the analysis of the long-term average AoI and provides a mathematical expression. In Section IV, an average AoI minimization problem is formulated subject to the energy and time constraints over the sensor nodes and MEC server. Section V proposes an SCA-based algorithm to solve the problem approximately and provides a convergence proof. In Section VI, we give some numerical results to evaluate the performance of our proposed algorithm and provides some insights for the network design. Furthermore, the notations are summarized in Table I.

II. System Model

Consider a WSN deployed in a region of interest (RoI) $\mathcal{Z}$ with K sensor nodes, an access point (AP) and an MEC server, as shown in Fig. 1. The MEC server also serves as the sink node in our paper. We denote these single-antenna sensor nodes as $s_k, k \in \mathcal{K} \triangleq \{1, 2, \ldots, K\}$, and the MEC server as s_0. The RoI $\mathcal{Z}$ can be partitioned into K zones, denoted by $\mathcal{Z}_k, k \in \mathcal{K}$, where the area of $\mathcal{Z}_k$ is A_k. The sensor node s_k is employed to monitor the environmental anomalies occurred in $\mathcal{Z}_k$, such as abnormal variation of temperature or humidity. As for the random anomalies, we assume that their occurrence time can be modeled by a Poisson process with intensity λ per unit area and unit time.

In our considered system, an asynchronous periodic sensing scheme is adopted. Specifically, the node s_k first senses the environment of $\mathcal{Z}_k$ and then generates a raw sampling packet,

TABLE I
SUMMARY OF NOTATIONS

Symbol	Definition
λ	Intensity of Poisson process
$\mathcal{Z}_k$	kth zone of interest
A_k	Area of $\mathcal{Z}_k$
s_k	kth sensor node
s_0	MEC server
τ_k	Sampling period for s_k
ρ_k	Sampling rate for s_k
E_{k0}	Initial energy of s_k
E_0	Initial energy of s_0
c_k	CPU frequency of s_k
Q_k	Computational workload for processing a raw packet at s_k
ℓ_{kn}	Local processing indicator of s_k in the nth sampling period
Δ_k	Average AoI on zone $\mathcal{Z}_k$
$T_{\min}$	Minimum WSN lifetime
$N_k(T)$	Arrival process of anomalies ahead of T
$\hat{N}_k(T)$	Departure process of packets ahead of T
$\bar{N}_k$	Average number of packets during T
q_k	Transmission outage probability of s_k
p_k	Transmission power of s_k
h_k	Channel gain between s_k and MEC server
κ_k	Energy conversion coefficient of CPU at s_k
D	Size of a raw packet in bits
d	Size of a processed packet in bits
R_k	Transmission rate of s_k

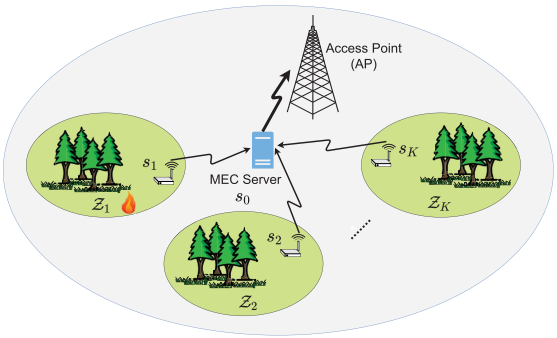

Fig. 1. Illustration of the system model with K sensor nodes, an MEC server, and an access point (AP).

where the sampling period for the kth node is τ_k, for all k. To reduce the traffic load of the network, data processing is necessary for all the packets before they are transferred to the AP. However, due to the strictly limited energy and computation capability of each sensor node, it is impractical to complete all the computational task at the nodes. In view of this, the MEC server s_0 is deployed in the system and leveraged to tradeoff the processing energy and the communication energy required by the sensor node s_k. Owing to deployment of s_0, each packet can be processed at the local node or remote MEC server. Compared to the sensor nodes that are distributed over a large geographical area, the MEC server s_0 can be generally deployed closer to the AP. For our considered system, all the packets are transferred to the MEC server first. Finally, the packets are forwarded to the AP by

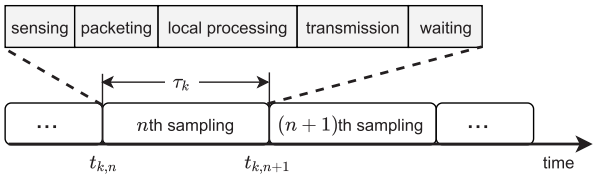

Fig. 2. Illustration of the sampling flow of the sensor node k with sampling period τ_k.

the MEC server. The operation flow is shown in Fig. 2, where $t_{k,n}$ is the start time of the nth sampling period for s_k.

For ease of exposition of offloading decision, we introduce a variable ℓ_{kn} as an indicator of the local processing for s_k at the nth sensing period. If s_k processes the packet locally at the nth sampling period, then $\ell_{kn} = 1$, otherwise, $\ell_{kn} = 0$. Besides, we denote the energy of s_k at the initial time as E_{k0} and denote the CPU frequency as c_k in terms of the CPU cycles per second. We assume that the MEC server has a larger battery capacity and higher computation power than the size-constrained sensor nodes, i.e., $E_0 > E_{k0}$, $c_0 > c_k, \forall k \in \mathcal{K}$, where E_0 and c_0 represents the initial energy and CPU frequency, respectively. Furthermore, we set the minimum lifetime of the WSN to be $T_{\min}$.

In light of the typical use cases in the internet of things (IoT) scenarios, it is assumed that the size of each packet is short, and a small bandwidth is enough for the wireless data transmission. Based on this consideration, the FDMA scheme is adopted in this work. We also assume the wireless link from s_k to s_0 is quasi-static, which means that the channel is constant during each sampling period and changes independently across different periods. In our setting, the Rayleigh fading is considered for the channel from s_k to s_0. Furthermore, for the case that the instantaneous channel state information (CSI) is not available at each sensor node, the transmission rate can not be adjusted adaptively based on the CSI. In consequence, we assume that each sensor node is allocated with equal bandwidth B for simplicity, and the kth node transmits packets with a fixed rate R_k, for all k.

To guarantee the performance of the sampling-based applications, such as wild fire forecasting, it is of utmost significance to improve the quality of the sample results in terms of freshness. In this paper, we adopt the AoI as the metric of timeliness of information, which would be applied in the DT network. The AoI is determined by the generation time of packets and the moment when the anomalies occurred. Therefore, the sampling rate together with the offloading decision have significant impacts on the AoI performance. In what follows, we will investigate the long-term average AoI of the considered system, and then improve the AoI performance by jointly optimizing the sampling rates and offloading decisions.

III. LONG-TERM AVERAGE AOI

In this section, we investigate the long-term AoI performance of the considered WSN system. As aforementioned, the sensor node s_k monitors the zone $\mathcal{Z}_k$ periodically and

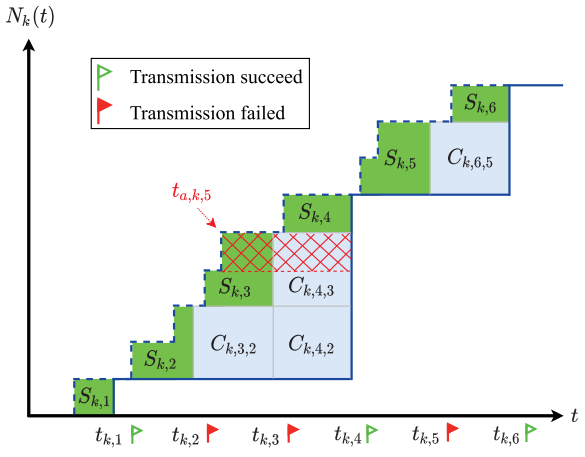

Fig. 3. Illustration of $N_k(t)$ (blue dashed line) and $\hat{N}_k(t)$ (blue solid line), where the 2nd, 3rd and 5th packet transmission from s_k are failed.

generates a packet after sensing in each sampling period. Since the periodic sampling scheme is adopted, the sensor node cannot sample the environment at the exact time when an anomaly occurs. Therefore, the information carried in the packet cannot be accurate, that is, the information is not fresh. In specific, the freshness of information is characterized by the time interval between the occurrence of anomaly and the moment when the next packet is successfully received. Hence, we should carefully characterize the freshness of information contained in the packets successfully received at s_0.

To this end, we investigate the arrival process of the anomalies in $\mathcal{Z}_k$ and the departure process of the packets from s_k to s_0. As illustrated in Fig. 3, the blue dashed polygonal line stands for the arrival process of the anomalies, denoted by $N_k(t)$. It is defined by the number of anomalies that occurred ahead of t in $\mathcal{Z}_k$, for all k. Due to the random channel fading, the successful transmission of a packet from s_k to s_0 is not guaranteed. As a result, s_0 can only obtain the latest information about $\mathcal{Z}_k$ based on the last successfully received packet from s_k. In view of this, we define the departure process as the generation process of the packets which are received successfully at s_0. Specifically, for the sensor node s_k, the packets departure process, denoted as $\hat{N}_k(t)$, is defined by

$$\hat{N}_k(t) = N_k(t_{k,j}),\ t_{k,n} \le t < t_{k,n+1},\ j \le n, \tag{1}$$

where $t_{k,j}$ denotes the sampling time of the last packet received successfully at s_0. $\hat{N}_k(t)$ is plotted in Fig. 3 with the blue solid line as an illustration.

Now let us focus on the AoI characterization of the packet received successfully at s_0. We define the AoI as the accumulation of time from the moment the anomaly occurs to the generation time of the next successfully received packet. As an example in Fig. 3, let $t_{a,k,5}$ denote the occurrence time of the 5th anomaly in $\mathcal{Z}_k$. Then, the AoI of the 5th anomaly can be expressed by $(t_{k,4} - t_{a,k,5})$. It can be readily shown that the AoI equals to the area of the red grid, as illustrated in Fig. 3. Thus, the total AoI on $\mathcal{Z}_k$ can be calculated by the area between the arrival and departure curves. It is analogous to the well-known queue accumulation polygon in the traffic flow theory. Based on the above analysis, the total AoI on $\mathcal{Z}_k$ during the period T can be expressed as

$$a_k(T) \triangleq \int_0^T \left(N_k(t) - \hat{N}_k(t)\right) \mathrm{d}t,\ \forall k, \tag{2}$$

where T is the operation duration of the sensor s_k.

Since the total AoI increases with T, we further define the average AoI by [27]

$$\Delta_k(T) \triangleq \frac{a_k(T)}{T} = \frac{1}{T}\int_0^T \left(N_k(t) - \hat{N}_k(t)\right) \mathrm{d}t. \tag{3}$$

Then, the long-term average AoI can be defined as

$$\Delta_k \triangleq \lim_{T\to\infty} \Delta_k(T),\ \forall k. \tag{4}$$

By analyzing the sampling scheme of the considered system, one readily notices that the staleness of information stems from the periodic sensing operation and the transmission outage due to the channel fading. Therefore, the total AoI can also be divided into two parts, namely the AoI due to sensing and the AoI due to communication, which are illustrated in Fig. 3 by the green and blue regions, respectively. We can calculate the two AoI parts separately and then obtain the total AoI on $\mathcal{Z}_k$. Denote by $S_{k,n}$ the AoI introduced by the sensing mode in the nth sampling period on $\mathcal{Z}_k$, and $C_{k,n,m}$ the AoI originated from the consecutive transmission outages from the mth to the $(n-1)$th transmissions of s_k. Hence, the long-term average AoI can be equivalently written as

$$\begin{aligned}\Delta_k &= \lim_{T\to\infty} \frac{1}{T}\int_0^T \left(N_k(t) - \hat{N}_k(t)\right) \mathrm{d}t \\ &= \lim_{T\to\infty} \frac{\bar{N}_k}{T} \cdot \frac{1}{\bar{N}_k}\left[\sum_{n=1}^{\bar{N}_k} S_{k,n} + \sum_{n=2}^{\bar{N}_k}\sum_{m=1}^{n-1} C_{k,n,m}\right] \\ &\triangleq \rho_k \mathbb{E}[S_k] + \rho_k \mathbb{E}[C_k],\end{aligned} \tag{5}$$

where $\bar{N}_k$ denotes the number of packets generated by s_k within T, $\rho_k \triangleq \frac{\bar{N}_k}{T} = \frac{1}{\tau_k}$ is the sampling rate of s_k, and

$$\mathbb{E}[S_k] \triangleq \lim_{\bar{N}_k\to\infty} \frac{1}{\bar{N}_k}\sum_{n=1}^{\bar{N}_k} S_{k,n}, \tag{6a}$$

$$\mathbb{E}[C_k] \triangleq \lim_{\bar{N}_k\to\infty} \frac{1}{\bar{N}_k}\sum_{n=2}^{\bar{N}_k}\sum_{m=1}^{n-1} C_{k,n,m}. \tag{6b}$$

In the following, we establish a proposition on the long-term average AoI Δ_k with detailed proof.

Proposition 1: The long-term average AoI on $\mathcal{Z}_k$ is given by

$$\Delta_k = \frac{\lambda A_k \tau_k}{2} + \lambda A_k \tau_k \frac{q_k}{1-q_k}, \tag{7}$$

where q_k denotes the outage probability of the wireless transmission from s_k to s_0, τ_k is the sampling interval, and A_k represents the geographical area of the region monitored by the sensor k, for all k.

Proof: Firstly, we focus on the expectation of S_k, i.e., $\mathbb{E}[S_k]$. Recall that the anomaly occurrence follows the Poisson

process with intensity λ. Then, based on the property of Poisson process, we have

$$\begin{aligned}\mathbb{E}[S_k] &= \mathbb{E}_i\Big[\mathbb{E}[S_{k,n}|N_k(t_{k,n}) - N_k(t_{k,n-1}) = i]\Big] \\ &= \mathbb{E}_i\left[\frac{i\tau_k}{2}\right] = \frac{\lambda A_k \tau_k^2}{2}. \end{aligned} \tag{8}$$

Then, let us consider $\mathbb{E}[C_k]$, which originates from the transmission outages of the packets from s_k to s_0. Specifically, $C_{k,n,m}$ is a random variable that depends on the previous transmissions, and we have

$$C_{k,n,m} = \begin{cases} 0, \text{ if there is at least one transmission succeed} \\ \quad \text{during } [t_{k,m}, t_{k,n-1}], \\ \tau_k\big(N_k(t_{k,m}) - N_k(t_{k,m-1})\big), \text{ otherwise.} \end{cases}$$

Due to the independence between transmissions, we can obtain

$$Pr(C_{k,n,m} = 0) = 1 - q_k^{n-m}, \tag{9a}$$

$$Pr\Big(C_{k,n,m} = \tau_k\big(N_k(t_{k,m}) - N_k(t_{k,m-1})\big)\Big) = q_k^{n-m}. \tag{9b}$$

Accordingly, we can rewrite $\mathbb{E}[C_k]$ as

$$\begin{aligned}\mathbb{E}[C_k] &\triangleq \lim_{\bar{N}_k\to\infty} \frac{1}{\bar{N}_k} \sum_{n=2}^{\bar{N}_k} \sum_{m=1}^{n-1} C_{k,n,m} \\ &= \lim_{\bar{N}_k\to\infty} \frac{1}{\bar{N}_k} \sum_{m=1}^{\bar{N}_k-1} \sum_{n=m+1}^{\bar{N}_k} C_{k,n,n-m} \\ &= \sum_{m=1}^{+\infty} \left[\lim_{\bar{N}_k\to\infty} \frac{1}{\bar{N}_k} \sum_{n=m+1}^{\bar{N}_k} C_{k,n,n-m}\right]. \end{aligned} \tag{10a}$$

It should be noted that $C_{k,n,n-m}$ is determined by the m consecutive transmissions before the nth sampling period. Thus, the random variables C_{k,n_1,n_1-m} and C_{k,n_2,n_2-m} with $n_1, n_2 > m$ and $n_1 \neq n_2$ are not necessarily independent. Specifically, C_{k,n_1,n_1-m} and C_{k,n_2,n_2-m} are independent if and only if $|n_1 - n_2| \geq m$. Hence, for ease of calculation of $\mathbb{E}[C_k]$, we define

$$\mathcal{C}_{k,m} \triangleq \{C_{k,n,n-m},\ \forall n\} = \cup_{j=1}^{m} \mathcal{X}_{k,m,j}, \tag{11}$$

where

$$\begin{aligned}\mathcal{X}_{k,m,j} \triangleq \Big\{C_{k,n,n-m}, \quad & n = (\imath+1)m + j, n \leq \bar{N}_k, \\ & \imath \in \Big\{0, 1, \ldots, \lfloor \tfrac{\bar{N}_k}{m} - 2 \rfloor\Big\}\Big\}. \end{aligned} \tag{12}$$

Note that

$$\lim_{\bar{N}_k\to\infty} |\mathcal{X}_{k,m,j}| = \left\lfloor \frac{\bar{N}_k}{m} \right\rfloor - 1,\ \forall k, m, j, \tag{13}$$

where $|\mathcal{X}_{k,m,j}|$ represents the cardinality of set $\mathcal{X}_{k,m,j}$. Thereby, $\lim_{\bar{N}_k\to\infty} \frac{1}{\bar{N}_k} \sum_{n=m+1}^{\bar{N}_k} C_{k,n,n-m}$ in (10a) can be expressed as

$$\begin{aligned}&\lim_{\bar{N}_k\to\infty} \frac{1}{\bar{N}_k} \sum_{n=m+1}^{\bar{N}_k} C_{k,n,n-m} \\ &= \lim_{\bar{N}_k\to\infty} \frac{|\mathcal{X}_{k,m,j}|}{\bar{N}_k} \cdot \frac{1}{|\mathcal{X}_{k,m,j}|} \sum_{j=1}^{m} \sum_{\imath=0}^{|\mathcal{X}_{k,m,j}|} C_{k,(\imath+1)m+j,\imath m+j} \\ &= \frac{1}{m} \sum_{j=1}^{m} \left[\lim_{|\mathcal{X}_{k,m,j}|\to\infty} \frac{1}{|\mathcal{X}_{k,m,j}|} \sum_{\imath=0}^{|\mathcal{X}_{k,m,j}|} C_{k,(\imath+1)m+j,\imath m+j}\right] \\ &= \frac{1}{m} \sum_{j=1}^{m} \mathbb{E}[X_{k,m,j}], \end{aligned} \tag{14}$$

where $X_{k,m,j} \in \mathcal{X}_{k,m,j}$ are i.i.d random variables.

Following (14), we further have

$$\begin{aligned}\mathbb{E}[X_{k,m,j}] &= \mathbb{E}_i\Big[\mathbb{E}[X_{k,m,j}|N_k(t_{k,n}) - N_k(t_{k,n-m}) = i]\Big] \\ &= \mathbb{E}_i[q_k^m i\tau_k] = q_k^m \lambda A_k \tau_k^2, \end{aligned} \tag{15}$$

where the second equality holds due to (9). Apparently, we can observe that $\mathbb{E}[X_{k,m,j}]$ is not related to j. Then, the mth term in (10a) is given by

$$\lim_{\bar{N}_k\to\infty} \frac{1}{\bar{N}_k} \sum_{n=m+1}^{\bar{N}_k} C_{k,n,n-m} = q_k^m \lambda A_k \tau_k^2. \tag{16}$$

Therefore, the average AoI introduced by the channel fading can be expressed as

$$\mathbb{E}[C_k] = q_k \lambda A_k \tau_k^2 + \cdots + q_k^m \lambda A_k \tau_k^2 + \cdots = \lambda A_k \tau_k^2 \frac{q_k}{1 - q_k} \tag{17}$$

Finally, the long-term average AoI Δ_k can be calculated as

$$\Delta_k = \frac{\lambda A_k \tau_k}{2} + \lambda A_k \tau_k \frac{q_k}{1 - q_k}, \tag{18}$$

which completes the proof. ■

As a consequence of the above proposition, we can obtain the following remark.

Remark 1: When q_k converges to 0, the average AoI on $\mathcal{Z}_k$ can be expressed as $\lambda A_k \tau_k/2$ that is similar to the conclusion in [27]. In this case, the staleness of information is only caused by the periodic sampling, and the average AoI is a linear function of τ_k. Apparently, if the sampling rate is high enough, there is no difference between the two curves as shown in Fig. 2, and the AoI becomes 0.

IV. Problem Formulation

In this section, a problem formulation will be provided for the WSN design based on the metric of the aforementioned average AoI. But, prior to the WSN design, we need to study the network from the perspectives of the energy and time models to characterize the system constraints.

A. Power and Energy Models of Sensor Node

1) Power Model: According to the composition of AoI, if q_k reaches 0, the AoI caused by the transmission outages vanishes. However, the smaller the outage probability q_k, the greater transmission power is required for s_k. Actually, the limited energy and the maximum transmission power hinder the improvement of the transmission performance of each sensor node. Here, we set the maximum transmission power as $p_{\max}$ for $s_k, \forall k \in \mathcal{K}$.

We define a transmission outage to occur if the transmission rate is larger than the channel capacity. Thus, we can establish

a relationship between the outage probability and the transmission power as following

$$\begin{aligned} q_k &= \Pr\left\{R_k > B\log_2\left(1+\frac{p_k g_k |h_k|^2}{N_0 B}\right)\right\} \\ &= \Pr\left\{|h_k|^2 < \frac{1}{p_k g_k} N_0 B(2^{\frac{R_k}{B}}-1)\right\}, \end{aligned} \tag{19}$$

where p_k denotes the transmission power of s_k, g_k represents the path loss from s_k to s_0, and h_k denotes the channel gain between s_k and s_0. Based on the assumption of Rayleigh fading channel, we have $|h_k|^2 \sim \exp(1)$. The explicit relationship between the transmission power p_k and the outage probability q_k can be given by

$$p_k = \frac{N_0 B(1-2^{\frac{R_k}{B}})}{g_k \ln(1-q_k)},\ \forall k \in \mathcal{K}. \tag{20}$$

Meanwhile, let $p_k = p_{\max}$, and thus the minimum of the outage probability of s_k is

$$q_k^{\min} = 1 - \exp\Big(-\frac{1}{p_{\max} g_k} N_0 B(2^{\frac{R_k}{B}}-1)\Big),\ \forall k. \tag{21}$$

2) Energy Model: The total energy consumption for a sensor node mainly consists of the energy expenditure for sensing, computation, and radio communication [28]. Since the interval sensing scheme is applied in our considered WSN, the sensing energy is not the major contributor to the total energy consumption [29]. In consequence, we will construct the energy consumption model of the sensor nodes from two aspects, namely the transmission part and computation part.

For each sensor node, the sizes of the raw packet and the processed packet are denoted by D and d in terms of bits, respectively. With consideration of the offloading decision, the transmission time of the nth packet from s_k to s_0 can be formulated as

$$T_{kn} = \tfrac{D+\ell_{kn}(d-D)}{R_k},\ \forall k, n. \tag{22}$$

Subsequently, the corresponding energy consumption for transmission is given by

$$E_{\text{Trans},k,n} = p_k T_{kn} = \tfrac{p_k[D+\ell_{kn}(d-D)]}{R_k},\ \forall k, n. \tag{23}$$

Next, we consider the energy consumption for computing. It is known that the energy expenditure for computation is highly related to the task load and the computation power of the CPU. The energy consumption of CPU can be simply modeled as κc_k^2 per CPU cycle for s_k, where κ is an energy conversion coefficient depending on the CPU architecture, and c_k represents the frequency of CPU at s_k [15], [30] Moreover, we denote the computational workload for processing a raw packet generated by s_k as Q_k. It can be defined by $Q_k = \alpha_k D$ in terms of the required CPU cycles, where α_k depends on the nature of the application [31], [32]. Without loss of generality, all the sensor nodes have the same hardware implementation and functions, and thus $\alpha_k = \alpha, \forall k \in \mathcal{K}$. Therefore, the energy consumption of the local computation for the nth packet can be computed as [15], [30]

$$E_{\text{Comp},k,n} = \kappa\alpha\ell_{kn} D c_k^2,\ \forall k, n. \tag{24}$$

To ensure s_k can operate within T, the energy consumption of s_k must satisfy the following constraint

$$\sum_{n=1}^{T\rho_k} (E_{\text{Trans},k,n} + E_{\text{Comp},k,n}) \le E_{k0},\ \forall k, \tag{25}$$

where $T\rho_k$ represents the total number of the packets generated by s_k during T. Then, by substituting (23) and (24) to (25), we have

$$\begin{aligned} &\sum_{n=1}^{T\rho_k}\left(\frac{p_k[D+\ell_{kn}(d-D)]}{R_k} + \kappa\alpha\ell_{kn}Dc_k^2\right) \\ &= T\rho_k\frac{p_k D}{R_k} + \frac{p_k(d-D)}{R_k}\sum_{n=1}^{T\rho_k}\ell_{kn} + \kappa\alpha D c_k^2\sum_{n=1}^{T\rho_k}\ell_{kn} \\ &= \|\boldsymbol{\ell}_k\|_1\Big(\frac{p_k d}{R_k} + \kappa\alpha D c_k^2\Big) + (T\rho_k - \|\boldsymbol{\ell}_k\|_1)\frac{p_k D}{R_k} \\ &= n_k\kappa\alpha D c_k^2 + \frac{p_k}{R_k}\big(T\rho_k D - n_k(D-d)\big), \end{aligned} \tag{26}$$

where $n_k \triangleq \|\boldsymbol{\ell}_k\|_1$.

In summary, the energy constraint on s_k can be written as

$$n_k\kappa\alpha D c_k^2 + \frac{p_k}{R_k}\big(T\rho_k D - n_k(D-d)\big) \le E_{k0},\ \forall k. \tag{27}$$

It is worth pointing out that the offloading schedule is characterized by a ratio of local computation, i.e., $n_k/(T\rho_k)$. Since we focus on designing an offline offloading schedule within the energy and time constraints of sensor nodes and MEC servers, the computation decision is not adjusted on a packet basis. Accordingly, all the schemes that can achieve the ratio are feasible.

B. Energy Model of MEC Server

As a result of the channel fading, some packets transmitted from s_k cannot be received successfully at s_0. If a packet cannot be decoded successfully, s_0 waits for the next packet from s_k. For the packets that can be successfully decoded, if needed, they will be processed at s_0 first and then transferred to the AP.

In view of the transmission outages and offloading decision, the average number of the packets that should be processed at s_0 is $\sum_{k=1}^{K}\sum_{n=1}^{T\rho_k}(1-q_k)(1-\ell_{kn})$. Accordingly, the energy used for the computation can be expressed as

$$E_{\text{Comp},0} = \kappa\alpha D c_0^2 \sum_{k=1}^{K}\sum_{n=1}^{T\rho_k}(1-q_k)(1-\ell_{kn}). \tag{28}$$

As for the average time consumption for packets transmission at s_0, it can be formulated as

$$T_0 = \frac{\sum_{k=1}^{K} T\rho_k(1-q_k)d}{R_0}. \tag{29}$$

Thus, the energy consumption for the transmission is given by

$$E_{\text{Trans},0} = p_0 T_0 = \frac{p_0 T d\sum_{k=1}^{K}\rho_k(1-q_k)}{R_0}. \tag{30}$$

Similar to (25), the energy constraint for s_0 is given by

$$E_{\text{Comp},0} + E_{\text{Trans},0} \le E_0. \tag{31}$$

Then, by substituting (28) and (30) to (31), we have

$$\kappa\alpha D c_0^2 \sum_{k=1}^{K}(T\rho_k - n_k)(1-q_k) + \frac{p_0 T d \sum_{k=0}^{K}\rho_k(1-q_k)}{R_0} \le E_0. \quad (32)$$

C. Time Model

We assume that the time used for the sensing and packetization is a constant, and we denote it as t_{sp}. Based on the offloading decision, each packet is needed to determine to process locally or remotely. Correspondingly, both the computation time and transmission time are contained in the sampling period, or just the transmission time should be considered. Hence, the constraints on sampling period τ_k can be readily expressed as

$$\begin{cases} \tau_k \ge \dfrac{d}{R_k} + \dfrac{\alpha D}{c_k} + t_{\text{sp}}, & \text{if local processing,} \\ \tau_k \ge \dfrac{D}{R_k} + t_{\text{sp}}, & \text{if remote processing.} \end{cases} \quad (33)$$

For brevity, it can be simplified as

$$\tau_k \ge \tau_k^{\min} \triangleq \max\left(\frac{d}{R_k} + \frac{\alpha D}{c_k} + t_{\text{sp}}, \frac{D}{R_k} + t_{\text{sp}}\right), \ \forall k. \quad (34)$$

Then, recalling to the definition of ρ_k, we can express the constraint over the sampling rate as

$$\rho_k \le \frac{1}{\tau_k^{\min}}, \ \forall k. \quad (35)$$

For the MEC server, since its computation power is high, the time consumed by processing a packet can be negligible compared to the corresponding transmission time [33]. Thus, only the transmission time should be taken into account. In our studied system, all the processed packets stored at s_0 need to be transmitted to the AP. Without loss of generality, the total transmission time should be no longer than the operation time T, and thus we have

$$\frac{\sum_{k=1}^{K} T\rho_k(1-q_k)d}{R_0} \le T. \quad (36)$$

Then, this constraint can be simplified as

$$\sum_{k=1}^{K}\rho_k(1-q_k) \le \frac{R_0}{d}. \quad (37)$$

Finally, from the perspective of the whole network lifetime, the operation time should be longer than $T_{\min}$. So we have

$$T \ge T_{\min}. \quad (38)$$

D. Formulation for AoI Minimization Problem

For the WSN aiming at collecting data, we want to keep the collected information as fresh as possible. Thereby, based on the aforementioned energy and time models, we can formulate the design of the WSN as an average AoI minimization problem as the following

$$\min_{\{\rho_k, n_k, q_k\}, T} \ \sum_{k=1}^{K}\Delta_k \quad (39a)$$

$$\text{s.t. } q_k^{\min} \le q_k < 1, \ \forall k, \quad (39b)$$

$$0 \le n_k \le T\rho_k, n_k \in \mathbb{N}, \ \forall k, \quad (39c)$$

$$(27), (32), (35), (37), \text{and } (38).$$

Let us focus on the lifetime constraint (38) first. It can be verified that the equality must hold at the optimal solution. Assume the constraint (38) is inactive at the optimal solution $(T^*, \{n_k^*, \rho_k^*, q_k^*\})$. We can always decrease T^* and $\{n_k^*\}$ proportionally such that $(T_{\min}, \{\frac{n_k^* T_{\min}}{T^*}, \rho_k^*, q_k^*\})$ is also the optimal solution to problem (39). Thus, we can remove the constraint (38) and denote the minimum lifetime as T for notational simplicity.

Next, we denote the transmit power of s_0 as p_0. For notational convenience, we define $p_0' \triangleq p_0/R_0$, and $p_k' \triangleq N_0 B(2^{\frac{R_k}{B}} - 1)/(g_k R_k)$. Furthermore, a simple transformation can be made for the average AoI (7) as below

$$\Delta_k = \frac{\lambda A_k \tau_k}{2} + \lambda A_k \tau_k \frac{q_k}{1-q_k} = -\frac{\lambda A_k}{2\rho_k} + \frac{\lambda A_k}{\rho_k(1-q_k)}. \quad (40)$$

So, problem (39) can be converted into problem (41) as shown below

$$\min_{\{\rho_k, n_k, q_k\}} \sum_{k=1}^{K}\left(-\frac{\lambda A_k}{2\rho_k} + \frac{\lambda A_k}{\rho_k(1-q_k)}\right) \quad (41a)$$

$$\text{s.t. } -\frac{p_k'}{\ln(1-q_k)}(T\rho_k D - n_k(D-d)) + \kappa\alpha D c_k^2 n_k \le E_{k0}, \ \forall k, \quad (41b)$$

$$\kappa\alpha D c_0^2 \sum\nolimits_{k=1}^{K}(T\rho_k - n_k)(1-q_k) + p_0' T d \sum\nolimits_{k=1}^{K}\rho_k(1-q_k) \le E_0, \quad (41c)$$

$$rho_k \le 1/\tau_k^{\min}, \ \forall k, \quad (41d)$$

$$\sum\nolimits_{k=1}^{K}\rho_k(1-q_k) \le R_0/d, \quad (41e)$$

$$q_k^{\min} \le q_k < 1, \ \forall k, \quad (41f)$$

$$0 \le n_k \le T\rho_k, n_k \in \mathbb{N}, \ \forall k. \quad (41g)$$

Before solving the problem, let us consider the relationship between the minimum lifetime and the corresponding AoI performance first. A lemma is provided as below.

Lemma 1: The optimal average AoI increases with the minimum network lifetime T monotonically. If the lifetime $T \to \infty$, then the average AoI approaches to infinite.

Proof: See Appendix A. ■

Remark 2: It should be noted that, when the minimum lifetime T is large enough, the time constraints (41d) *and* (41e) *need not to be considered due to the low sampling rate. Then, by analyzing the problem without time constraints, it can be shown that the average AoI increases linearly in T. Besides, $\rho_k \propto \frac{1}{T}$, while the outage probability and ratio of local computation are almost constant when T is large.*

Remark 3: For comparison, we consider a WSN without the aid of the MEC server. Obviously, only the energy and

time constraints over the sensor nodes need to be taken into account. Since all the packets are processed locally, the energy and time constraints over s_k can be rewritten as

$$T\rho_k\kappa\alpha D c_k^2 + \frac{p_k}{R_k} T\rho_k d \le E_{k0},\ \forall k, \tag{42a}$$

$$\Big(\frac{d}{R_k} + \frac{\alpha D}{c_k} + t_{\rm sp}\Big) \le \frac{1}{\rho_k},\ \forall k. \tag{42b}$$

Thereby, the AoI minimization problem (41) *can reduce to*

$$\min_{\{\rho_k, q_k\}, T} \sum_{k=1}^{K} \Delta_k \tag{43a}$$

$$\text{s.t.} \quad q_k^{\min} \le q_k < 1,\ \forall k, \tag{43b}$$

$$(38), (42a), \text{and } (42b).$$

In view of the same reason to (41)*, we can also remove the constraint* (38) *and drop the subscript from $T_{\min}$. Then, by substituting* (20) *into* (42a)*, problem* (43) *can be recast as*

$$\min_{\{\rho_k, q_k\}} \ \sum_{k=1}^{K} \left(-\frac{\lambda A_k}{2\rho_k} + \frac{\lambda A_k}{\rho_k (1-q_k)} \right) \tag{44a}$$

$$\text{s.t.} \quad q_k^{\min} \le q_k < 1,\ \forall k \in \mathcal{K}, \tag{44b}$$

$$T\rho_k\kappa\alpha D c_k^2 - \frac{p_k'}{\ln(1-q_k)} T\rho_k d \le E_{k0},\ \forall k, \tag{44c}$$

$$\rho_k \le 1/\Big(\frac{d}{R_k} + \frac{\alpha D}{c_k} + t_{\rm sp}\Big),\ \forall k, \tag{44d}$$

where $p_k' \triangleq N_0 B(2^{\frac{R_k}{B}} - 1)/(g_k R_k), \forall k$.

Let us turn back to problem (41). It can be verified that problem (41) is a nonconvex optimization problem and difficult to solve optimally. Specifically, the difficulty lies in the fact that variables ρ_k and q_k couple in two different forms, and the same is true for n_k and q_k.

Remark 4: We can extend the transmission scheme to the case that the processed packets can be sent directly to the AP. For this transmission scheme, the corresponding problem formulation is given by

$$\min_{\{\rho_k, n_k, q_k\}} \ \sum_{k=1}^{K} \left(-\frac{\lambda A_k}{2\rho_k} + \frac{\lambda A_k}{\rho_k (1-q_k)} \right) \tag{45a}$$

$$\text{s.t.} \quad -\frac{p_k^{\rm M}}{\ln(1-q_k)} (T\rho_k - n_k) D - \frac{p_k^{\rm A}}{\ln(1-q_k)} n_k d + \kappa\alpha D c_k^2 n_k \le E_{k0},\ \forall k, \tag{45b}$$

$$(p_0' d + \kappa\alpha D c_0^2) \sum\nolimits_{k=1}^{K} (T\rho_k - n_k)(1-q_k) \le E_0, \tag{45c}$$

$$\rho_k \le 1/\tau_k^{\min},\ \forall k, \tag{45d}$$

$$\sum_{k=1}^{K} (T\rho_k - n_k)(1-q_k) \le \frac{R_0 T}{d}, \tag{45e}$$

$$q_k^{min} \le q_k < 1,\ \forall k, \tag{45f}$$

$$0 \le n_k \le T\rho_k, n_k \in \mathbb{N},\ \forall k, \tag{45g}$$

where $p_k^{\rm M} \triangleq N_0 B(2^{\frac{R_k}{B}} - 1)/(g_k^{\rm M} R_k)$ *and* $p_k^{\rm A} \triangleq N_0 B(2^{\frac{R_k}{B}} - 1)/(g_k^{\rm A} R_k)$. $g_k^{\rm M}$ *and* $g_k^{\rm A}$ *represent the path loss from the node k to the MEC server and AP, respectively. Apparently, the challenge of solving the problem* (45) *is the same as that of solving (40). Therefore, we only focus on solving the problem (40) in this paper for brevity.*

In the next section, we resort to the SCA method and then an SCA-based algorithm is proposed to solve problem (41) approximately. Besides, for the special case in (44), a closed-form optimal solution is provided.

V. Algorithm Design

Due to the couplings among the variables, it is challenging to solve problem (41) with global optimality. However, it is noteworthy that the intractable couplings in the problem are of product forms. This observation prompts us to leverage the main idea of the geometric programming to transform the problem into a tractable form by a change of variables. In the following, two efficient algorithms are proposed to solve problems (41) and (44), respectively.

A. Algorithm Design for Solving Problem (41)

Inspired by the geometric programming, we introduce the variables x_k and y_k to the problem, where $x_k \triangleq -\ln(1-q_k)$ and $\rho_k \triangleq e^{y_k}$. By performing the variable substitution, problem (41) can be rewritten as

$$\min_{\{x_k, y_k, n_k\}} \ \sum_{k=1}^{K} \frac{\lambda A_k}{2} \left(-e^{-y_k} + 2e^{x_k - y_k} \right) \tag{46a}$$

$$\text{s.t.} \quad n_k x_k + \tfrac{p_k'}{C_k} (T D e^{y_k} - (D-d) n_k) \le \tfrac{E_{k0}}{C_k} x_k,\ \forall k, \tag{46b}$$

$$\sum_{k=1}^{K} e^{y_k - x_k} \le \alpha_1 + \alpha_0 \sum_{k=1}^{K} n_k e^{-x_k}, \tag{46c}$$

$$\sum_{k=1}^{K} e^{y_k - x_k} \le R_0/d, \tag{46d}$$

$$y_k \le -\ln(\tau_k^{\min}),\ \forall k, \tag{46e}$$

$$x_k \ge 0,\ \forall k, \tag{46f}$$

$$0 \le n_k \le T e^{y_k}, n_k \in \mathbb{N},\ \forall k, \tag{46g}$$

where $\alpha_0 \triangleq \frac{C_0}{(C_0 T + p_0' T d)}$ and $\alpha_1 \triangleq \frac{E_0}{(C_0 T + p_0' T d)}$. However, solving the problem (46) is still challenging due to the non-convex objective and the constraints (46b) and (46c).

To deal with the challenges, an algorithm based on the SCA method is proposed to approximately solve problem (46). First, it is easy to see that the coupling between variables n_k and x_k appears of the product form in the constraints (46b). In light of this, the slack variables $\{z_k\}$ are introduced to the problem aiming at converting the non-convex constraints into tractable forms. To this end, let $n_k x_k \le z_k^2$, and then the constraints (46b) can be rewritten as

$$\frac{z_k^2}{n_k} \ge x_k,\ \forall k, \tag{47a}$$

$$z_k^2 + \tfrac{p_k'}{C_k} (T D e^{y_k} - (D-d) n_k) \le \tfrac{E_{k0}}{C_k} x_k,\ \forall k. \tag{47b}$$

In consequence, problem (46) can be transformed into the following problem

$$\min_{\{x_k,y_k,n_k,z_k\}} \sum_{k=1}^{K} \frac{\lambda A_k}{2}\left(-e^{-y_k}+2e^{x_k-y_k}\right) \quad (48)$$
$$\text{s.t.} \quad (46c)-(46g), (47a), \text{and } (47b).$$

It should be noted that the problem (48) is equivalent to the problem (46). Therefore, we focus on how to solve the problem (48) in the following. Specifically, the proof of equivalence lies in the tightness of the constraint (47a) at the optimal solution to the problem (48). It can be readily proved by using the contradiction argument, and we omit this proof due to the page limitations.

To proceed, we turn to the energy constraint (46c). For this constraint, we can apply the SCA method to approximate it to a convex constraint. Using the first-order Taylor expansion of e^{-x} at $\bar{x}$, we have

$$e^{-x} \geq e^{-\bar{x}} - e^{-\bar{x}}(x-\bar{x}) = (1+\bar{x})e^{-\bar{x}} - xe^{-\bar{x}}, \quad (49)$$

where the equality holds if and only if $x=\bar{x}$. Thus, the constraint (46c) can be guaranteed if the following constraint holds

$$\sum_{k=1}^{K}\left(\alpha_0 n_k x_k e^{-\bar{x}_k}+e^{y_k-x_k}\right) \leq \alpha_1 + \alpha_0 \sum_{k=1}^{K} n_k(1+\bar{x}_k)e^{-\bar{x}_k}. \quad (50)$$

Notice that $n_k x_k$ appears in (50). Since the constraint (47a) holds with equality at the optimal solution to problem (48), we can replace $n_k x_k$ in the constraint (50) with z_k^2. Then, an approximated convex constraint can be obtained as

$$\sum_{k=1}^{K}\left(\alpha_0 z_k^2 e^{-\bar{x}_k}+e^{y_k-x_k}\right) \leq \alpha_1 + \alpha_0 \sum_{k=1}^{K} n_k(1+\bar{x}_k)e^{-\bar{x}_k}. \quad (51)$$

As for the other non-convex constraints, the first-order Taylor expansion can be also applied to obtain tractable approximations. For brevity, we omit the details here.

In our setting, the network lifetime $T_{\min}$ is large enough so that the optimal solution $\{n_k^*\}$ is also large in general. In view of this, for simplicity, we remove the integer constraints over $\{n_k\}$ from (46g). When the optimal solution $\{n_k^\star\}$ is obtained by solving (48) without integer constraints, we can round $\{n_k^\star\}$ to the nearest integers to obtain an approximate solution.

Through the above operations, the problem (48) can be approximated to a convex optimization problem at the point $\{\bar{x}_k, \bar{z}_k, \bar{n}_k\}$ as following

$$\min_{\{x_k,y_k,n_k,z_k\}} \sum_{k=1}^{K} \frac{\lambda A_k}{2}(-e^{-\bar{y}_k}+e^{\bar{y}_k}(y_k-\bar{y}_k)+2e^{x_k-y_k}) \quad (52a)$$

$$\text{s.t.} \quad \frac{2\bar{z}_k}{\bar{n}_k}z_k - \frac{\bar{z}_k^2}{\bar{n}_k^2}n_k \geq x_k, \ \forall k, \quad (52b)$$

$$0 \leq n_k \leq T\left(e^{\bar{y}_k}+e^{\bar{y}_k}(y_k-\bar{y}_k)\right), \ \forall k, \quad (52c)$$

$$(46d), (46e), (46f), (47b), \text{and } (51).$$

Algorithm 1 SCA-Based Method for Solving Problem (46)

1: **Initialization**: Given $T_{\min}$, $\boldsymbol{q}^0$, $\boldsymbol{\rho}^0 = 1/\boldsymbol{\tau}^{\min}$, an accuracy tolerance ϵ, and set iteration index $r=0$.
2: **if** (41e) is violated
3: $\quad \boldsymbol{\rho}^0 := \frac{R_0}{(d\sum_{k=1}^{K}\rho_k^0(1-q_k^0))}\boldsymbol{\rho}^0$
4: **end if**
5: $\bar{\boldsymbol{x}}^0 = -\ln(1-\boldsymbol{q}^0)$
6: **while**
7: $\quad \boldsymbol{n}^0 = T_{\min}\boldsymbol{\rho}^0$
8: $\quad$ **if** (41b) or (41c) is violated
9: $\quad\quad \boldsymbol{\rho}^0 := \boldsymbol{\rho}^0/2$
10: $\quad$ **else**
11: $\quad\quad$ **break**
12: $\quad$ **end if**
13: **end while**
14: $\bar{\boldsymbol{y}}^0 = \ln(\boldsymbol{\rho}^0), \bar{\boldsymbol{n}}^0 = T_{\min}\boldsymbol{\rho}^0, \{\bar{z}_k^0 = \sqrt{\bar{x}_k^0 \bar{n}_k^0}\}$, where $\bar{z}_k^0$ denotes the n-th element of $\bar{\boldsymbol{z}}$;
15: **repeat**
16: $\quad$ set $r := r+1$
17: $\quad$ solve problem (52), and obtain the optimal solution $\{\boldsymbol{x}^{r*}, \boldsymbol{y}^{r*}, \boldsymbol{z}^{r*}, \boldsymbol{n}^{r*}\}$;
18: $\quad$ update $\bar{\boldsymbol{x}}^r = \boldsymbol{x}^{r*}, \bar{\boldsymbol{y}}^r = \boldsymbol{y}^{r*}, \bar{\boldsymbol{z}}^r = \boldsymbol{z}^{r*}, \bar{\boldsymbol{n}}^r = \boldsymbol{n}^{r*}$;
19: **until** the decrease of the objective in problem (46) is smaller than ϵ.

In summary, we can approximately solve the problem (48) by solving the problem (52) iteratively. The details of the SCA-based method is summarized in Algorithm 1. The convergence of our proposed algorithm can be guaranteed by the following lemma.

Lemma 2: The sequence of the objective value of the problem (46)*, which is obtained by applying Algorithm 1, is nonincreasing. The convergence of Algorithm 1 can be guaranteed.*

Proof: For notational clarity, we define $\boldsymbol{v}^r \triangleq (\boldsymbol{x}^r, \boldsymbol{y}^r, \boldsymbol{z}^r, \boldsymbol{n}^r)$, and the objective value of the problem (46) as $f(\boldsymbol{v}^r)$ for an optimal solution $\boldsymbol{v}^r$ at the rth iteration. Due to the application of the first-order Taylor expansion, the original objective (46a) is approximated by an upper bound function (52a). For convenience, we denote the objective (52a) as $\bar{f}(\boldsymbol{v}|\boldsymbol{v}^r)$ at the rth iteration. Besides, we have

$$\bar{f}(\boldsymbol{v}|\boldsymbol{v}^r) \geq f(\boldsymbol{v}), \quad (53)$$

where the equality holds if and only if $\boldsymbol{v}=\boldsymbol{v}^r$.

Based on the above definitions and the fact that all the iterations are feasible, it is not hard to see that

$$f(\boldsymbol{v}^{r+1}) \leq \bar{f}(\boldsymbol{v}^{r+1}|\boldsymbol{v}^r) \leq \bar{f}(\boldsymbol{v}^r|\boldsymbol{v}^r) = f(\boldsymbol{v}^r). \quad (54)$$

Therefore, the objective value of the problem (46) is non-increasing by applying our proposed algorithm. Moreover, since the objective value is lower bounded by 0, the proposed algorithm can converge. ■

Remark 5: It is worth mentioning that the initial problem (41) *becomes a convex optimization problem on $\{\rho_k, n_k\}$ with given outage probability sequence $\{q_k\}$. Hence, it can be solved efficiently by some optimization solvers, such as the*

CVX [34]. Likewise, for fixed $\{\rho_k, n_k\}$*, the problem* (41) *can be also transformed into a convex optimization problem of* q_k*. In view of this, we can solve the problem* (41) *by adopting the alternating optimization (AO) method to optimize* $\{\rho_k, n_k\}$ *and* $\{q_k\}$ *alternately. However, the simulation results show that our proposed SCA-based method can outperform the AO-based method.*

B. Algorithm Design for Solving Problem (44)

It should be noted that the problem (44) can be also solved by adopting the SCA method. However, the optimal solution can be obtained by exploiting the structure of the problem (44). Similar to the method for solving (41), we can apply the variable substitution, and thus the problem (44) can be recast as the following

$$\min_{\{x_k, y_k\}} \quad \sum_{k=1}^{K} \frac{\lambda A_k}{2}\left(-e^{-y_k} + 2e^{x_k - y_k}\right) \tag{55a}$$

$$\text{s.t.} \quad x_k \geq x_k^{\min} \triangleq -\ln(1 - q_{\min}),\ \forall k, \tag{55b}$$

$$y_k \leq y_k^{\max} \triangleq \ln\left(1/\left(\frac{d}{R_k} + \frac{\alpha D}{c_k}\right)\right),\ \forall k, \tag{55c}$$

$$TC_k e^{y_k}\left(x_k + \frac{p_k'}{C_k}d\right) \leq E_{k0}x_k,\ \forall k, \tag{55d}$$

where $C_k \triangleq \kappa\alpha D c_k^2$. Owing to the structure of the above problem, a closed-form optimal solution can be obtained as shown in the following lemma.

Lemma 3: Considering s_k*, the optimal solution is* $(x_k^{\min}, y_k^{\max})$ *if the constraint* (55d) *can be guaranteed with* $x_k = x_k^{\min}, y_k = y_k^{\max}$*. Otherwise, we have the optimal solution* $y_k^* = \ln\left(\frac{E_{k0}x_k^*}{T(C_k x_k^* + p_k' d)}\right)$*, where* x_k^* *can be obtained by solving the following equation with the bisection method.*

$$2e^{x_k}\left(C_k x_k^2 + p_k' d(x_k - 1)\right) + p_k' d = 0. \tag{56}$$

Proof: See Appendix B. ∎

VI. Simulation Results

In this section, we provide some numerical results to evaluate the performance of the proposed algorithms and give some insights for the network design. Without loss of generality, we consider $K = 6$ sensor nodes in the system and assume all the nodes have the same CPU frequency and initial energy. Each sensor node monitors a circular region with a radius $r = 30$ m, and the distances between the sensor nodes to the MEC server are 150 m. A distance-dependent path loss model is adopted as following

$$PL(d) = L_0\left(\frac{d}{d_0}\right)^{-\beta}, \tag{57}$$

where $L_0 = 30$ dB is the path loss at the reference distance $d_0 = 1$ m, d represents the distance between the transmitter and receiver, and $\beta = 3.5$ is the path-loss exponent. Moreover, we set $\alpha = 800$ and $\kappa = 10^{-28}$ [15], [31].

In the first example, we give some simulation results to illustrate the impact of the energy of the sensor nodes and

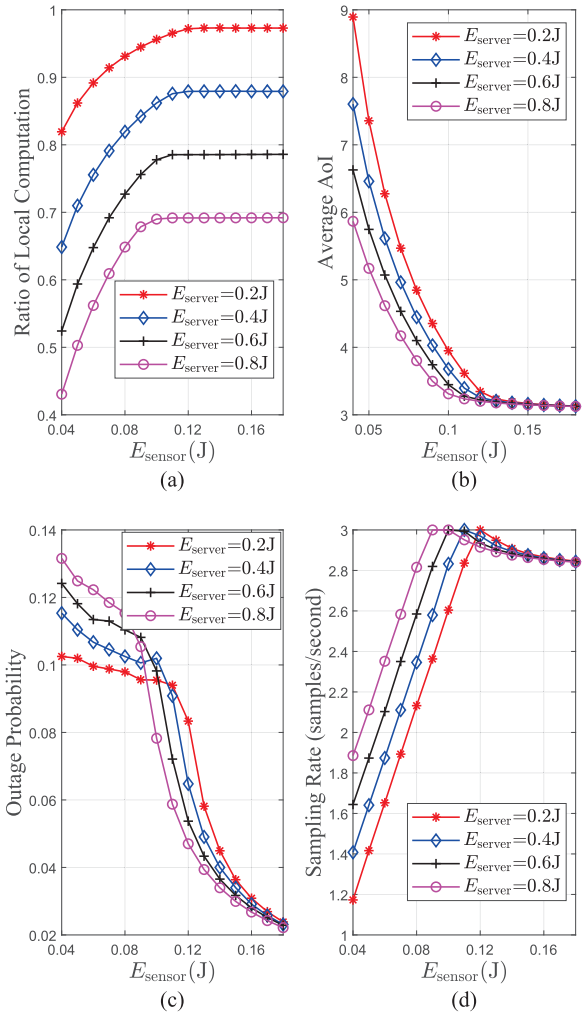

Fig. 4. Ratio of local computation (a), average AoI (b), outage probability (c), and sampling rate (d) versus the initial energy of sensor node E_{sensor}.

MEC server on the network performance. As can be seen in Fig. 4(a), the sensor nodes process a large percentage of the packets if the initial energy E_{server} of s_0 is limited. Besides, the ratio of local computation increases with the increased energy of the sensor nodes. In Fig. 4(b), we can see that the average AoI decreases with the increase of the nodes' energy. However, due to the limitation of computation capability, the average AoI is no longer decreasing even if E_{sensor} is large enough.

Then, we consider the outage probability and the sampling rate. As illustrated in Fig. 4(c), we can observe that the outage probability q_{sensor} decreases almost monotonically with the increasing energy of the sensor nodes. More interestingly, the variation of the outage probability can be divided into two phases with increased E_{sensor}. By observing Fig. 4(c) and (d), we know that the sensor nodes tend to increase the sampling rates rather than decreasing the outage probabilities in the first phase. To make sense of it, let us turn to the objective (41a). It can be readily verified that the average AoI is a monotonically decreasing function of ρ_{sensor} and $(1 - q_{\text{sensor}})$. Due to the fact that $(1 - q_{\text{sensor}}) \in (0, 1)$, compared to

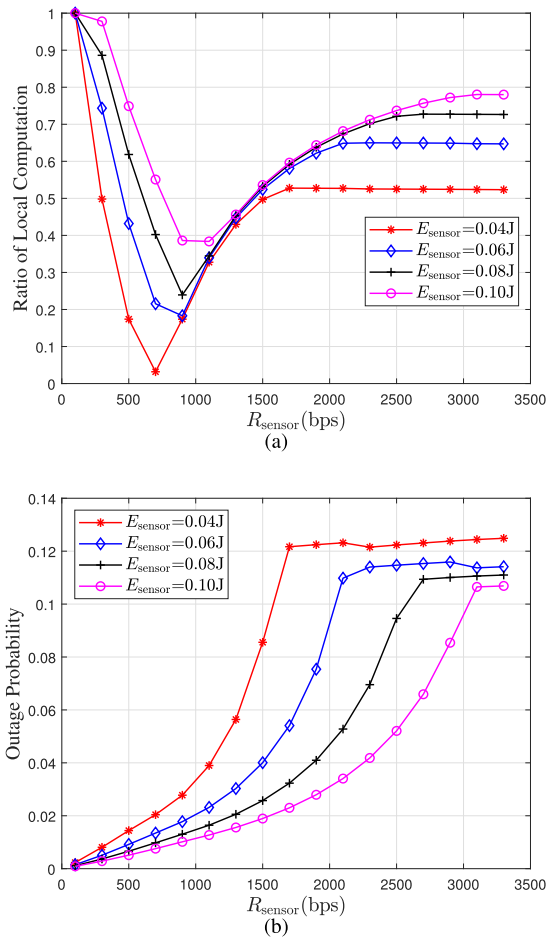

Fig. 5. Ratio of local computation (a), and outage probability (b) versus the transmission rate of sensor node R_{sensor}.

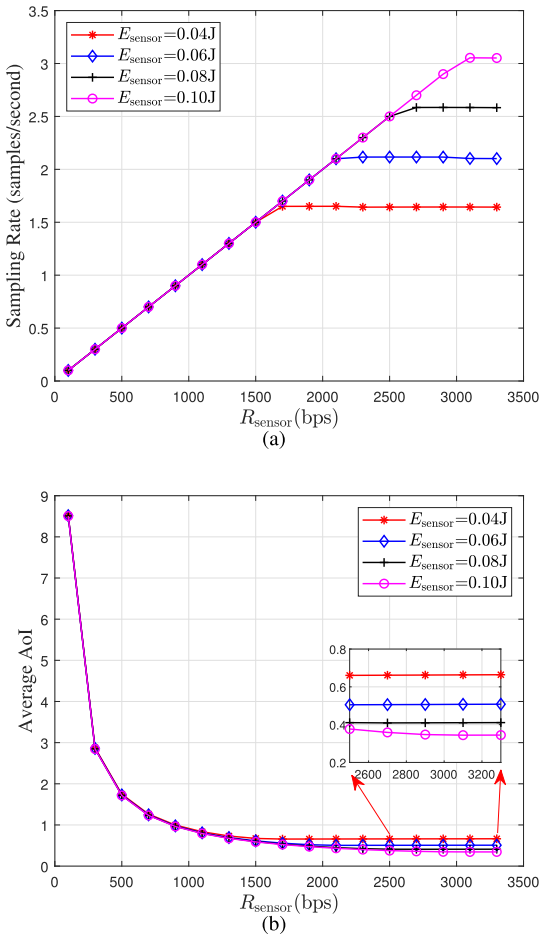

Fig. 6. Sampling rate (a), and average AoI (b) versus the transmission rate of sensor node R_{sensor}.

increasing the sampling rates, decreasing q_{sensor} cannot provide a remarkable performance gain for the AoI of the network. By contrast, despite the sufficient energy of the sensor nodes in the second phase, the sampling rates cannot further increase due to the limitation of computation power. Thus, the most effective way to reduce the AoI is to decrease the outage probability.

Turning now to the impact of the transmission rate of the sensor nodes on the AoI performance. In Fig. 5(a), one can observe that the proportion of local computation can be divided into three parts with the increase of the transmission rate. When the transmission rate is too small, the sensor nodes process all the packets locally. By further increasing the transmission rate, the ratio of local computation reduces first and then increases. For ease of explanation, we should focus on the left-hand side of the constraint (41b). It can be reformulated as

$$n_k\left(\kappa\alpha D c_k^2+\frac{p_k'(D-d)}{\ln(1-q_k)}\right)-\frac{p_k' T\rho_k D}{\ln(1-q_k)}. \tag{58}$$

The monotonicity of (58) to n_k depends on the term $\kappa\alpha D c_k^2+\frac{p_k'}{\ln(1-q_k)}(D-d)$. Therefore, the outage probability q_{sensor} has a significant influence on the offloading decision. When the transmission rate R_{sensor} is small, the sampling rate ρ_{sensor} is bounded by the constraint (41d). As a consequence, the sensor nodes prefer to decrease the outage probabilities for improving the AoI performance. With a small q_{sensor}, the energy consumption of the sensor nodes decreases monotonically with n_k, and thus all the packets are processed locally. However, with the increase of R_{sensor}, the sensor nodes would increase the sampling rates at the cost of higher outage probabilities to obtain better AoI performance. It implies that q_{sensor} can reach the threshold such that the monotonicity of the energy consumption w.r.t n_k changes. Consequently, the sensor nodes reduce the ratio of local computation dramatically, which results in the second phase in Fig. 5(a). Then, when the transmission rate becomes large and the ratio of local computation is small, the energy of the MEC server becomes a bottleneck. In consequence, the proportion of the local computation gradually increase. From Fig. 5(b), we see that the outage probability increase with the transmission rate until the energy of sensor nodes becomes a bottleneck. Furthermore, as shown in Fig. 5(b), there is a clear tendency that the sensor nodes with less energy sacrifice more transmission performance to guarantee the AoI performance.

To proceed, we consider the variation of the sampling rate and average AoI with the increase of sensor transmission rate as shown in Fig. 6. In Fig. 6(a), with small transmit rate, the

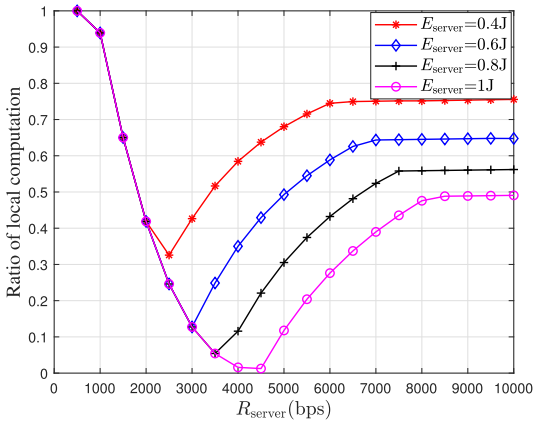

Fig. 7. Ratio of local computation versus R_{sensor}.

sampling rates are the same for the cases of different sensor energy, which mainly lies in the constraints (41d). For a high transmit rate, the energy of the sensor nodes becomes a new bottleneck, which results in a high sampling rate for the case of the sufficient sensor energy. In Fig. 6(b), it is observed that the almost same AoI performance can be achieved when R_{sensor} is small no matter how much the energy of sensor nodes is. Additionally, it is evidently that a low transmit rate leads to a large AoI. Thereby, we should set a little high transmit rate in practice to obtain good AoI performance.

We also consider the impact of transmission rate of MEC server as shown in Fig. 7. There are also three phases for the ratio of local computation. In the first stage, sensor nodes process all the computation tasks because of a low outage probability, which is similar to the first phase in Fig. 5(a). The cause of low outage probability lies in the time constraint $\sum_{k=1}^{K}\rho_k(1-q_k) \le \frac{R_{\text{server}}}{d}$. When the transmission rate of the MEC server R_{server} is low enough, the value of $\rho_k(1-q_k)$ is bounded due to the constraint (41e). Let us turn to the objective $\sum_{k=1}^{K}\left(-\frac{\lambda A_k}{2\rho_k}+\frac{\lambda A_k}{\rho_k(1-q_k)}\right)$. With a fixed value of $\rho_k(1-q_k)$, we can know that an effective method of reducing the AoI is to decrease ρ_k. The reason is that the objective is a decreasing function with respect to ρ_k when $\rho_k(1-q_k)$ is bounded. Correspondingly, a low outage probability q_k can be realized.

Next, the comparison of the AoI performance for our proposed methods is illustrated in Fig. 8(a). It is observed that, for the AO-based method, the monotonicity of average AoI with respect to E_{sensor} cannot be guaranteed. The underlying reason is that, for fixed $\{q_k\}$, the power constraint (41c) is generally tight with optimized $\{\rho_k, n_k\}$. In the next iteration, the smaller outage probabilities cannot be obtained due to the tight constraint (41c). Accordingly, the AO-based method converges very fast, and its performance is highly dependent on the choice of initial point. In contrast, due to the obtained approximate solution, the SCA-based method has room to continue reducing the average AoI. Additionally, we can see that a near-optimal solution can be obtained by applying the proposed SCA-based method compared to the benchmark of exhaustive method. In Fig. 8(b), the proposed SCA-based method can converge within 4 iterations, while the AO-based method stops at the second iteration.

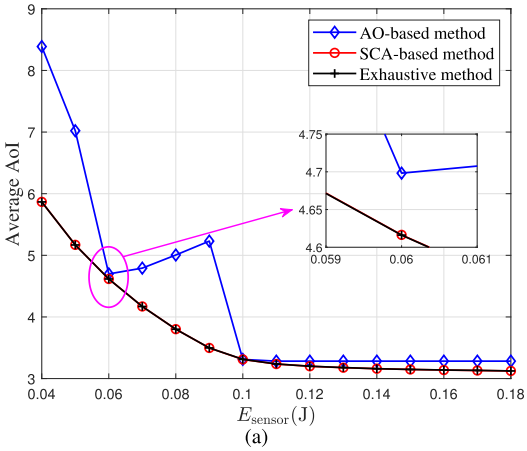

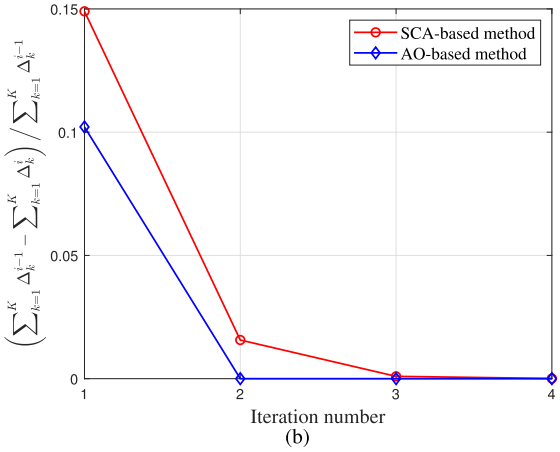

Fig. 8. (a) Methods comparison for different E_{sensor}, (b) iterative performance.

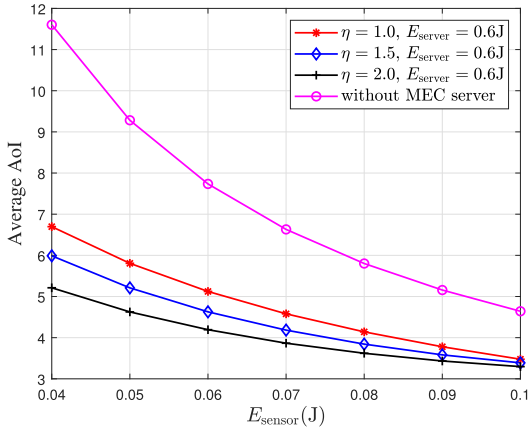

Fig. 9. AoI performance comparison for systems with and without the MEC server.

To exhibit the benefits of the MEC server, we take the case of non-homogeneous areas into account. Specifically, we define a scaling factor by $\eta = A_k/A_{k+1}$ for $k = 1, \ldots, K-1$, where the total area $\sum_{k=1}^{K} A_k$ is a constant. In Fig. 9, we consider the WSN without and with the MEC server, respectively. η is set to be 1, 1.5, and 2 for the case with the MEC server. When the sensor nodes monitor the zones with different areas, the MEC server can play

a significant role to balance the workload in the network across different sensor nodes. From Fig. 8, one can readily see that the AoI performance can be improved in non-homogeneous case compared to the homogeneous case, especially when η is large. In contrast, when there is no MEC server, the AoI minimization problem can be divided into K independent subproblems. The offloading schedule and outage probability are the smae for different η. Besides, it is shown that the MEC server can improve the network performance remarkably when the sensors have limited energy.

VII. Conclusion

In this paper, we considered a WSN that monitors the environment in a given zone and provided a definition of AoI. By analyzing operating mode of the WSN, a closed-form expression of the long-term average AoI was obtained. Then, an average AoI minimization problem was formulated subject to the energy and time constraints on the sensor nodes and MEC server. It's difficult to solve this problem due to the variables coupling. To tackle this problem, we proposed an SCA-based algorithm to solve the problem approximately with the guaranteed convergence. Moreover, a WSN without the MEC server was also investigated, and a closed-form solution was provided. Finally, the simulation results showed the efficiency of our proposed SCA-based algorithm and demonstrated that the proposed algorithm outperforms the AO-based approach. Additionally, a remarkable AoI performance gain can be achieved by integrating the WSN with MEC technique.

Appendix A
Proof of Lemma 1

Proof: With a given minimum lifetime T_1, we denote the optimal solution to problem (41) as $(\boldsymbol{n}^*, \boldsymbol{q}^*, \boldsymbol{\rho}^*)$. For ease of exposition, the objective value of problem (41) is denoted as $f_{T_1}(\boldsymbol{q}, \boldsymbol{\rho})$ for given lifetime T_1 and a feasible solution $(\boldsymbol{n}, \boldsymbol{q}, \boldsymbol{\rho})$, where $\boldsymbol{n}$ is not reflected in the objective. Furthermore, to facilitate the development of the proof, we assume that there is a new lifetime constraint $T \leq T_2$ for the network, where $T_2 < T_1$.

By a simple analysis, we know that the left sides of the constraints (41b) and (41c) are increasing functions of T. Besides, as the variables representing the number of packets processed locally, $\{n_k\}$ are time-dependent as shown in (41g). Based on the above results, we can easily construct a feasible solution $(\boldsymbol{n}^\star, \boldsymbol{q}^*, \boldsymbol{\rho}^*)$ to problem (41) with lifetime T_2 such that the constraints (41b) and (41c) can be satisfied, where $\boldsymbol{n}^\star \triangleq T_2/T_1\boldsymbol{n}^*$. Specifically, it should be noted that both the constraints (41b) and (41c) hold with the strict inequalities. As a result, we can always further increase the sampling rate and obtain a new feasible solution $(\boldsymbol{n}^\star, \boldsymbol{\rho}^\star, \boldsymbol{q}^*)$, where $\boldsymbol{\rho}^\star \succeq \boldsymbol{\rho}^*$. More importantly, based on the structure of the objective, we have

$$f_{T_2}(\boldsymbol{\rho}^\star, \boldsymbol{q}^*) < f_{T_1}(\boldsymbol{\rho}^*, \boldsymbol{q}^*). \tag{59}$$

So far, we have shown that the optimal average AoI increases monotonically with T.

Then, we consider the average AoI in the case of $T \to \infty$. Based on the constraints (41g), the following equation must hold

$$\kappa\alpha D c_0^2 \sum_{k=1}^{K} (T\rho_k - n_k)(1 - q_k) \geq 0. \tag{60}$$

Meanwhile, with consideration of the constraint (41c) and the fact of $E_0 < \infty$, we can draw a conclusion that $\sum_{k=1}^{K} \rho_k^*(1 - q_k^*) \to 0$ when T converges to infinity.

Next, let us turn to the objective, and we can rewrite it as $\sum_{k=1}^{K} \frac{\lambda A_k(1+q_k)}{2\rho_k(1-q_k)}$. Therefore, we have

$$\sum_{k=1}^{K} \frac{\lambda A_k(1+q_k^*)}{2\rho_k^*(1-q_k^*)} > \sum_{k=1}^{K} \frac{\lambda A_k}{2\rho_k^*(1-q_k^*)} \to \infty, \tag{61}$$

which implies that the average AoI converges to infinity when $T \to \infty$. ■

Appendix B
Proof of Lemma 2

Proof: We first focus on the objective of problem (55). It can be expressed as

$$\sum_{k=1}^{K} \frac{\lambda A_k}{2} \big((2e^{x_k} - 1)e^{-y_k}\big), \tag{62}$$

which is a monotonically decreasing function of y_k due to $(2e^{x_k} - 1) > 1$ for $x_k > 0$. Obviously, it also monotonically increases with x_k. Therefore, in order to minimize the objective, we should increase y_k and decrease x_k at the same time. Note that there is no coupling among the sensor nodes, and thus we just focus on s_k.

When the initial energy of s_k is enough, it is readily to obtain the optimal solution, i.e., $x_k^* = x_k^{\min}$, and $y_k^* = y_k^{\max}$. It also implies that we should increase the sampling rate and transmission power as much as possible if the energy is sufficient.

When E_{k0} is not large enough, s_k cannot support the maximum sampling rate and transmission power. Then, it can be readily proved that the constraint (55d) must hold with equality at the optimal solution. Therefore, we have

$$e^{y_k} = \frac{E_{k0}x_k}{TC_kx_k + Tp'_kd}, \ \forall k. \tag{63}$$

Then, by substituting (63) to (62), the objective can be recast as

$$\sum_{k=1}^{K} (2e^{x_k} - 1)\frac{TC_kx_k + Tp'_kd}{E_{k0}x_k}. \tag{64}$$

Next, by analyzing its second derivative, we know that the objective is a convex function of x_k. Hence, the optimal solution x_k^* can be obtained by finding the point where the first derivative equals 0 if the point locates in the feasible set of x_k. Here, recall that y_k is an increasing function with respected to x_k in (63). Thus, the feasible set of x_k is $[x_k^{\min}, x_k^{\max}]$, where

$$x_k^{\max} = \begin{cases} Tp'_kde^{y_k^{\max}}/(E_{k0} - TC_ke^{y_k^{\max}}), & \text{if } e^{y_k^{\max}} < \frac{E_{k0}}{TC_k}, \\ +\infty, & \text{otherwise.} \end{cases} \tag{65}$$

In light of this, we solve the following equation first

$$f(x_k) \triangleq 2e^{x_k}\left(C_k x_k^2 + p_k' d(x_k - 1)\right) = -p_k' d, \ \forall k. \quad (66)$$

It is readily to prove that $f(x_k)$ is an increasing function with respect to x_k when $x_k > 0$. The bisection method can be applied to obtain the solution to (66), and the solution is denoted as $x_k^\star$. If $x_k^\star < x_k^{\min}$, we have $x_k^* = x_k^{\min}$. When $x_k^\star > x_k^{\max}$, there is $x_k^* = x_k^{\max}$. That completes the proof. ■

REFERENCES

[1] H. X. Nguyen, R. Trestian, D. To, and M. Tatipamula, "Digital twin for 5G and beyond," *IEEE Commun. Mag.*, vol. 59, no. 2, pp. 10–15, Feb. 2021.

[2] Y. Wu, K. Zhang, and Y. Zhang, "Digital twin networks: A survey," *IEEE Internet Things J.*, vol. 8, no. 18, pp. 13789–13804, Sep. 2021.

[3] P. Jia, X. Wang, and X. Shen, "Digital-twin-enabled intelligent distributed clock synchronization in industrial IoT systems," *IEEE Internet Things J.*, vol. 8, no. 6, pp. 4548–4559, Mar. 2021.

[4] Y. Lu, S. Maharjan, and Y. Zhang, "Adaptive edge association for wireless digital twin networks in 6G," *IEEE Internet Things J.*, vol. 8, no. 22, pp. 16219–16230, Nov. 2021.

[5] H. Huang, T. Gong, R. Zhang, L.-L. Yang, J. Zhang, and F. Xiao, "Intrusion detection based on k-coverage in mobile sensor networks with empowered intruders," *IEEE Trans. Veh. Technol.*, vol. 67, no. 12, pp. 12109–12123, Dec. 2018.

[6] A. Argyriou and O. Alay, "Distributed estimation in wireless sensor networks with an interference canceling fusion center," *IEEE Trans. Wireless Commun.*, vol. 15, no. 3, pp. 2205–2214, Mar. 2016.

[7] S. Karimi-Bidhendi, J. Guo, and H. Jafarkhani, "Energy-efficient node deployment in heterogeneous two-tier wireless sensor networks with limited communication range," *IEEE Trans. Wireless Commun.*, vol. 20, no. 1, pp. 40–55, Jan. 2021.

[8] S. Guo, C. Wang, and Y. Yang, "Joint mobile data gathering and energy provisioning in wireless rechargeable sensor networks," *IEEE Trans. Mobile Comput.*, vol. 13, no. 12, pp. 2836–2852, Dec. 2014.

[9] M. Noori and M. Ardakani, "Lifetime analysis of random event-driven clustered wireless sensor networks," *IEEE Trans. Mobile Comput.*, vol. 10, no. 10, pp. 1448–1458, Oct. 2011.

[10] Y. Yun, Y. Xia, B. Behdani, and J. C. Smith, "Distributed algorithm for lifetime maximization in a delay-tolerant wireless sensor network with a mobile sink," *IEEE Trans. Mobile Comput.*, vol. 12, no. 10, pp. 1920–1930, Oct. 2013.

[11] T. X. Tran, A. Hajisami, P. Pandey, and D. Pompili, "Collaborative mobile edge computing in 5G networks: New paradigms, scenarios, and challenges," *IEEE Commun. Mag.*, vol. 55, no. 4, pp. 54–61, Apr. 2017.

[12] Z. Ke, S. Leng, Y. He, S. Maharjan, and Y. Zhang, "Mobile edge computing and networking for green and low-latency Internet of Things," *IEEE Commun. Mag.*, vol. 56, no. 5, pp. 39–45, May 2018.

[13] C. Wang, C. Liang, F. R. Yu, Q. Chen, and L. Tang, "Computation offloading and resource allocation in wireless cellular networks with mobile edge computing," *IEEE Trans. Wireless Commun.*, vol. 16, no. 8, pp. 4924–4938, Aug. 2017.

[14] O. Muñoz, A. Pascual-Iserte, and J. Vidal, "Optimization of radio and computational resources for energy efficiency in latency-constrained application offloading," *IEEE Trans. Veh. Technol.*, vol. 64, no. 10, pp. 4738–4755, Oct. 2015.

[15] S. Mao, S. Leng, S. Maharjan, and Y. Zhang, "Energy efficiency and delay tradeoff for wireless powered mobile-edge computing systems with multi-access schemes," *IEEE Trans. Wireless Commun.*, vol. 19, no. 3, pp. 1855–1867, Mar. 2020.

[16] R. D. Yates, Y. Sun, D. R. Brown, S. K. Kaul, E. Modiano, and S. Ulukus, "Age of information: An introduction and survey," *IEEE J. Sel. Areas Commun.*, vol. 39, no. 5, pp. 1183–1210, May 2021.

[17] H. Tang, P. Ciblat, J. Wang, M. Wigger, and R. D. Yates, "Cache updating strategy minimizing the age of information with time-varying files' popularities," in *Proc. IEEE Inf. Theory Workshop (ITW)*, Apr. 2021, pp. 1–5.

[18] X. Wu, X. Li, J. Li, P. C. Ching, V. C. M. Leung, and H. V. Poor, "Caching transient content for IoT sensing: Multi-agent soft actor-critic," *IEEE Trans. Commun.*, vol. 69, no. 9, pp. 5886–5901, Sep. 2021.

[19] A. Baknina, O. Ozel, J. Yang, S. Ulukus, and A. Yener, "Sending information through status updates," in *Proc. IEEE Int. Symp. Inf. Theory (ISIT)*, Jun. 2018, pp. 2271–2275.

[20] Y. Xiao and Y. Sun, "A dynamic jamming game for real-time status updates," in *Proc. IEEE Conf. Comput. Commun. Workshops (INFOCOM WKSHPS)*, Apr. 2018, pp. 354–360.

[21] A. E. Kalør and P. Popovski, "Minimizing the age of information from sensors with common observations," *IEEE Wireless Commun. Lett.*, vol. 8, no. 5, pp. 1390–1393, Oct. 2019.

[22] A. Valehi and A. Razi, "Maximizing energy efficiency of cognitive wireless sensor networks with constrained age of information," *IEEE Trans. Cogn. Commun. Netw.*, vol. 3, no. 4, pp. 643–654, Dec. 2017.

[23] N. Hirosawa, H. Iimori, K. Ishibashi, and G. T. F. D. Abreu, "Minimizing age of information in energy harvesting wireless sensor networks," *IEEE Access*, vol. 8, pp. 219934–219945, 2020.

[24] I. Krikidis, "Average age of information in wireless powered sensor networks," *IEEE Wireless Commun. Lett.*, vol. 8, no. 2, pp. 628–631, Apr. 2019.

[25] M. Moltafet, M. Leinonen, and M. Codreanu, "Worst case age of information in wireless sensor networks: A multi-access channel," *IEEE Wireless Commun. Lett.*, vol. 9, no. 3, pp. 321–325, Mar. 2020.

[26] S. Zhang, J. Li, H. Luo, J. Gao, L. Zhao, and X. S. Shen, "Towards fresh and low-latency content delivery in vehicular networks: An edge caching aspect," in *Proc. 10th Int. Conf. Wireless Commun. Signal Process. (WCSP)*, Oct. 2018, pp. 1–6.

[27] M. Bastopcu and S. Ulukus, "Who should Google scholar update more often?" in *Proc. IEEE Conf. Comput. Commun. Workshops (INFOCOM WKSHPS)*, Jul. 2020, pp. 696–701.

[28] B. Han, D. Zhang, and T. Yang, "Energy consumption analysis and energy management strategy for sensor node," in *Proc. IEEE Int. Conf. Inf. Autom. (ICIA)*, Jun. 2008, pp. 211–214.

[29] T. O. John, H. C. Ukwuoma, S. Danjuma, and M. Ibrahim, "Energy consumption in wireless sensor network," *Energy*, vol. 7, no. 8, pp. 63–67, 2016.

[30] X. Hu, K.-K. Wong, and K. Yang, "Wireless powered cooperation-assisted mobile edge computing," *IEEE Trans. Wireless Commun.*, vol. 17, no. 4, pp. 2375–2388, Apr. 2018.

[31] C. You, K. Huang, and H. Chae, "Energy efficient mobile cloud computing powered by wireless energy transfer," *IEEE J. Sel. Areas Commun.*, vol. 34, no. 5, pp. 1757–1771, May 2016.

[32] W. Zhang, Y. Wen, K. Guan, D. Kilper, H. Luo, and D. O. Wu, "Energy-optimal mobile cloud computing under stochastic wireless channel," *IEEE Trans. Wireless Commun.*, vol. 12, no. 9, pp. 4569–4581, Sep. 2013.

[33] M. Min, L. Xiao, Y. Chen, P. Cheng, D. Wu, and W. Zhuang, "Learning-based computation offloading for IoT devices with energy harvesting," *IEEE Trans. Veh. Technol.*, vol. 68, no. 2, pp. 1930–1941, Feb. 2019.

[34] M. Grant and S. Boyd. (Mar. 2014). *CVX: MATLAB Software For Disciplined Convex Programming, Version 2.1*. [Online]. Available: http://cvxr.com/cvx

Guangyang Zhang (Graduate Student Member, IEEE) received the B.S. degree in communication engineering from Beijing Jiaotong University (BJTU), China, in 2019, where he is currently pursuing the Ph.D. degree with the State Key Laboratory of Rail Traffic Control and Safety. His current research interests include age of information (AoI) and IRS-aided wireless communications.

Chao Shen (Member, IEEE) received the B.S. degree in communication engineering and the Ph.D. degree in signal and information processing from Beijing Jiaotong University (BJTU), Beijing, China, in 2003 and 2012, respectively.

He was a Visiting Scholar at the University of Maryland, College Park, MD, USA, from 2014 to 2015, and The Chinese University of Hong Kong, Shenzhen, China, from 2017 to 2018. He has been an Associate Professor with the State Key Laboratory of Rail Traffic Control and Safety, BJTU, since 2012. He has been working as a Senior Research Scientist with the Shenzhen Research Institute of Big Data, Shenzhen, since 2022. His current research interests include large-scale network optimization, ultrareliable and low-latency communication (URLLC), and integrated sensing and communication (ISAC) for B5G/6G communications.

Qingjiang Shi (Member, IEEE) received the Ph.D. degree in electronic engineering from Shanghai Jiaotong University, Shanghai, China, in 2011.

From September 2009 to September 2010, he visited Prof. Z.-Q. (Tom) Luo's Research Group at the University of Minnesota, Twin Cities. In 2011, he was a Research Scientist at Bell Laboratories, China. He was at the School of Information and Science Technology, Zhejiang Sci-Tech University, in 2012. From February 2016 to March 2017, he was a Research Fellow at Iowa State University, USA. Since March 2018, he has been currently a Full Professor with the School of Software Engineering, Tongji University. He is also with the Shenzhen Research Institute of Big Data. He has published more than 70 IEEE journals and filed about 30 national patents. His interests include algorithm design and analysis with applications in machine learning, signal processing, and wireless networks. He was a recipient of the Huawei Outstanding Technical Achievement Award in 2021, the Second Prize of Huawei Technical Cooperation Achievement Transformation Award in 2022, the Golden Medal from the 46th International Exhibition of Inventions of Geneva in 2018, the First Prize of Science and Technology Award from the China Institute of Communications in 2017, the National Excellent Doctoral Dissertation Nomination Award in 2013, the Shanghai Excellent Doctorial Dissertation Award in 2012, and the Best Paper Award from the IEEE Personal, Indoor and Mobile Radio Communications (PIMRC)'09 Conference. He was an Associate Editor of the IEEE TRANSACTIONS ON SIGNAL PROCESSING.

Bo Ai (Fellow, IEEE) received the M.S. and Ph.D. degrees from Xidian University, Xi'an, China, in 2002 and 2004, respectively. He was an Excellent Post-Doctoral Research Fellow at Tsinghua University, Beijing, China, in 2007. He is currently a Professor and an Advisor of Ph.D. candidates with Beijing Jiaotong University, Beijing, where he is also the Deputy Director of the State Key Laboratory of Rail Traffic Control and Safety. He is also with the Engineering College, Armed Police Force, Xi'an. He has authored or coauthored six books and 270 scientific research papers, and holds 26 invention patents in his research areas. His interests include the research and applications of orthogonal frequency-division multiplexing techniques, high-power amplifier linearization techniques, radio propagation and channel modeling, global systems for mobile communications for railway systems, and long-term evolution for railway systems.

Zhangdui Zhong (Fellow, IEEE) received the B.E. and M.S. degrees from Beijing Jiaotong University, Beijing, China, in 1983 and 1988, respectively.

He is currently a Professor and an Advisor of Ph.D. candidates with Beijing Jiaotong University, where he is also currently a Chief Scientist of the State Key Laboratory of Rail Traffic Control and Safety. He is also the Director of the Innovative Research Team, Ministry of Education, Beijing, and the Chief Scientist of the Ministry of Railways, Beijing. He is also an Executive Council Member of the Radio Association of China, Beijing, and the Deputy Director of the Radio Association, Beijing. He has authored or coauthored seven books, five invention patents, and over 200 scientific research papers in his research area. His research interests include wireless communications for railways, control theory and techniques for railways, and GSM-R systems. His research has been widely used in railway engineering, such as the Qinghai-Xizang railway, Datong-Qinhuangdao Heavy Haul railway, and many high-speed railway lines in China. He was a recipient of the Mao Yisheng Scientific Award of China, the Zhan TianYou Railway Honorary Award of China, and the Top 10 Science/Technology Achievements Award of Chinese Universities.